Shadow-free motorized capsule enables accurate beam positioning and sectorized OCT imaging of the esophagus

López-Marín, Antonio; Springeling, Geert; Beurskens, Robert; Van Beusekom, Heleen; Van Der Steen, Antonius; Koch, Arjun D.; Bouma, Brett E.; Huber, Robert A.; Van Soest, Gijs; Wang, Tianshi

PROCEEDINGS OF SPIE

SPIEDigitalLibrary.org/conference-proceedings-of-spie

Shadow-free motorized capsule enables accurate beam positioning and sectorized OCT imaging of the esophagus

López-Marín, Antonio, Springeling, Geert, Beurskens, Robert, van Beusekom, Heleen, van der Steen, Antonius, et al.

SPIE.

Shadow-free motorized capsule enables accurate beam positioning and sectorized OCT imaging of the esophagus

Antonio López-Marín[a], Geert Springeling[a], Robert Beurskens[a], Heleen van Beusekom[a], Antonius F.W. van der Steen[a,b,c], Arjun D. Koch[a], Brett E. Bouma[d,e], Robert Huber[f], Gijs van Soest[a], and Tianshi Wang[a]

[a]Erasmus University Medical Center, P. O. Box 2040, Rotterdam 3000 CA, The Netherlands; [b]Shenzhen Institutes of Advanced Technology, Chinese Academy of Sciences, Shenzhen, 518005, China; [c]Department of Imaging Science and Technology, Delft University of Technology, Delft, 2600 AA, The Netherlands; [d]Wellman Center for Photomedicine, Harvard Medical School and Massachusetts General Hospital, 40 Blossom Street, Boston, Massachusetts 02114, USA; [e]Harvard-MIT Program in Health Sciences and Technology, Cambridge, Massachusetts 02139, USA; [f]Institut für Biomedizinische Optik, Universität zu Lübeck, Lübeck, 23562, Germany

ABSTRACT

In this study, we demonstrate a 12x36 mm motorized capsule for OCT imaging of the esophagus. The capsule produces unobstructed images by using a distal reflector design, thus avoiding shadow caused by the motor wires. The motor synchronous control enables three working modes: circumferential imaging, angular sector imaging and accurate beam positioning. Distortion artifacts shown in the sector imaging were found to be induced by velocity changes of the motor. We specifically characterized the motor speed and found a symmetric and repeatable behavior during sector scanning. Resampling of the sector images A-lines was carried out to achieve uniform angular spacing according to the measured speed profile. Also, distortion between consecutive sector frames was corrected using image registration to achieve stable imaging.

Keywords: Optical Coherence Tomography, optical imaging, light beams, magnetic fields, gradient index lenses, image reconstruction

1. INTRODUCTION

Optical Coherence Tomography (OCT) is an imaging technique able to generate cross-sectional images of the internal micro structure of tissue samples.[1,2] Using an imaging catheter, endoscopic OCT can generate images of luminal tissue with millimeter penetration depth and micrometer resolution. Specifically designed for the gastrointestinal tract, tethered capsules have been demonstrated as an alternative to conventional video endoscopy, avoiding sedation and thus reducing patient discomfort.[3,4] A distal motorized design allows for a reduced rotational distortion, accurate beam scanning,[5,6] and laser marking procedures.[7] However, wires of distal motors partially block the scanning area, producing image shadows. This issue might become critical when abnormal tissue is coincidentally blocked in the image.

Previously, we demonstrated the first motorized capsule that can generate shadow-free OCT images of the esophagus.[8] In addition, using a synchronous motor design, the capsule allows circumferential imaging and features the absolute positioning and sector imaging modes. Using the sector scanning mode, the capsule can visualize the region of interest (ROI) locally and potentially apply a laser mark in the ROI by holding the laser beam upon it. Even though morphological features can be recognized in the sectorized images, distortion artifacts induced by the acceleration and deceleration of the motor can also be observed.

Former studies have demonstrated that lateral velocity can be derived from speckle decorrelation methods, and compensation can be applied accordingly in post processing.[9,10] In this study, we characterized the speed profile of the sector scanning mode, analyzed the distortion in the image and finally applied image reconstruction to compensate such distortion. Moreover, we implemented an image registration method to further compensate the misalignment between consecutive OCT frames to achieve stable visualization of sector imaging.

2. METHODS

2.1 Motorized capsule

Fig. 1 shows the photo and schematic diagram of the tethered capsule. In order to avoid shadow artifacts in the image, the Gradient Refractive Index (GRIN) lens and the micromotor were laid side by side rather than facing each other as in conventional designs. Since two additional distal reflectors were used, the optical length is longer than in former capsules. A customized GRIN lens (Go!Foton, United States) with a longer focal length of 20 mm focuses the laser beam approximately 2.0 mm away from the capsule surface. The reflectivity of the silver-coated reflectors (Edmund, United States) was measured as > 93.6%. Total power losses contribute to -2.3 dB loss in sensitivity compared to an overall measured sensitivity of 96 dB for the capsule-OCT system.
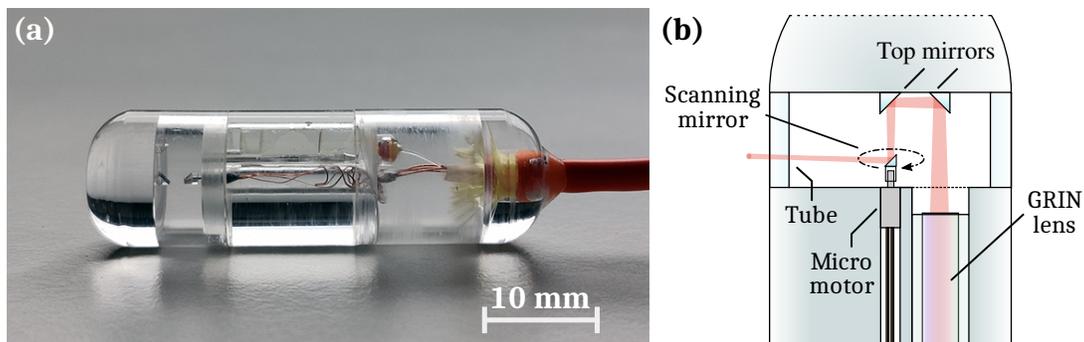
Figure 1. **Shadow-free motorized capsule**. (a) Photo and (b) schematic diagram of the optics setup of the capsule; GRIN: Gradient refractive index. The top mirrors face both motor and GRIN probe, redirecting the laser beam from the lens to the tissue.

2.2 Motor control and characterization

The motor used in this capsule is a 2-phase, 4-pole synchronous micromotor (Kinetron, the Netherlands) driven by two sinusoidal current signals with a 90° shift. Because it is synchronous, the rotational speed is always proportional to the frequency of the driving signals. Also, the angular position of the permanent magnet rotor is synchronized to the magnetic field generated by the two sinusoidal currents. This feature enables three advanced working modes of the capsule: absolute positioning, circumferential scanning and sector scanning. Absolute positioning of the laser beam can be realized by controlling the phase of the driving currents. Circumferential scanning is performed by driving the channel signals periodically. Sector scanning works as an extension of absolute position, varying the driving signals around a center angular position θ within a specific range $\pm d\theta$ (Fig. 2). We developed a virtual instrument (LabVIEW, United States) to control the motor in real time.
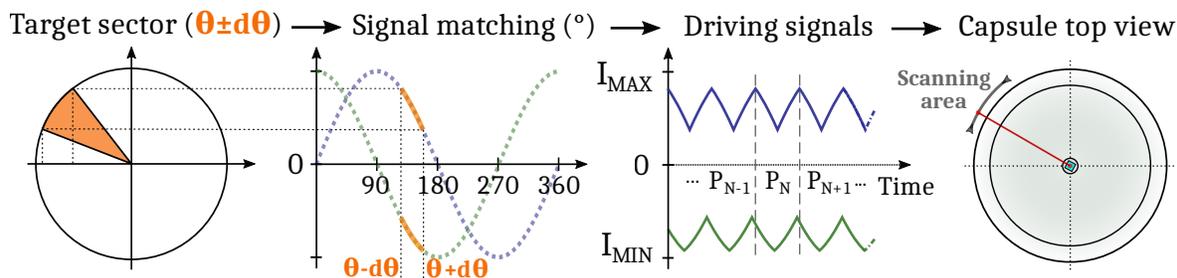
Figure 2. **Operation flow for the sector scanning mode**. Input angular values (phase) are matched to specific phase values of the sinusoidal driving signals. Periodic driving of the signals segments enables the sectorized scanning mode; $P_\#$: signal period.

We characterized these three modes using a home-built setup (Fig. 3), the details of which can be found in our previous study.[11] The capsule was placed in the center of a cylindrical tube, which has 360 angular markings (in 1° steps) and 180 slits (in 2° steps). This setup allows us to measure both the instantaneous velocity of the micromotor and the position of the laser beam emitting from the capsule. In this study, we specifically characterized the speed profile in sectorized scanning to find out the link between the image distortion and non-uniform rotation of the micromotor.
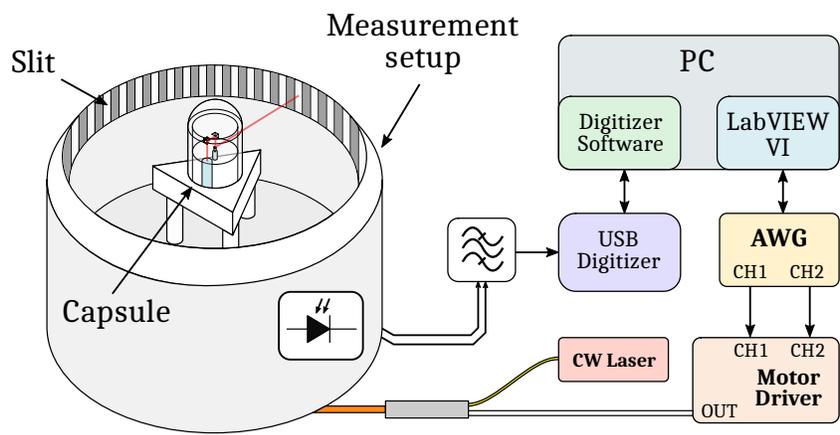
Figure 3. **Motorized capsule characterization setup**. CW: Continuous wave; AWG: Arbitrary waveform generator.

2.3 Image processing for distortion compensation

Distortion in sector imaging was analyzed and compensated in two steps. In the first step, the speed distortion of individual frames is compensated through after speckle decorrelation analysis. In the second step, we extend the compensation to multiple frames through image registration methods. A flowchart of the whole process can be found in Fig. 4.
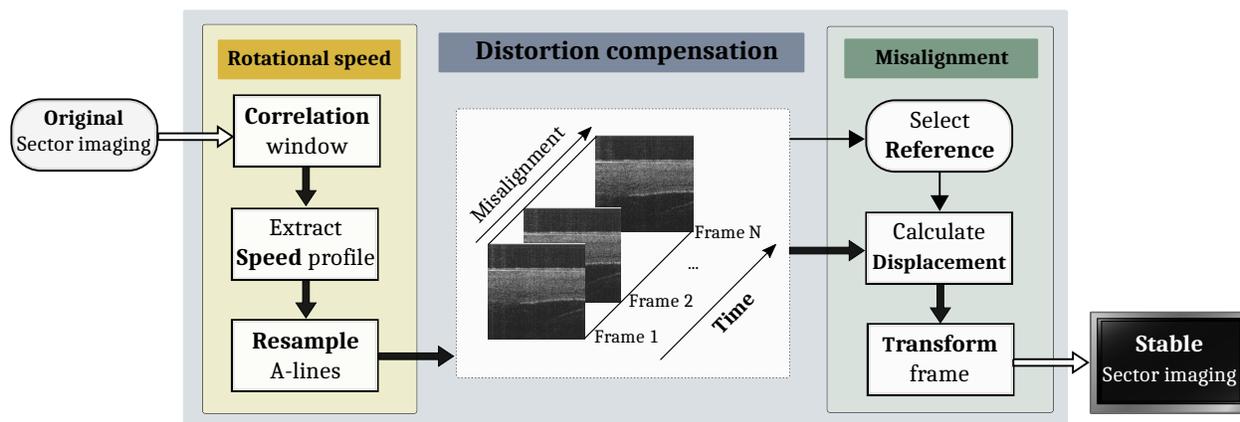
Figure 4. **Sector imaging compensation workflow**. Frames are individually compensated to achieve stable imaging.

To compensate for distortion within a single frame, we extracted the relative speed of the motor during sector scanning using speckle decorrelation methods. We first applied a correlation window (21 x 500 pixels) that laterally sweeps the visible tissue area. In each window, the Pearson correlation coefficient (PCC) between A-lines was calculated and averaged. After applying a normalization, a low-pass filtering and a cumulative sum, the resulting signal represents the reciprocal of the angular density of A-lines. Based on the velocity profile, a nearest-neighbor resampling was finally applied to achieve uniform lateral distribution of A-lines.

To achieve stable sectorized imaging with multiple frames, we further compensated the frame-to-frame distortion by implementing an image registration algorithm, which makes use of functions that are part of the Image Processing Toolbox (MATLAB, United States). The algorithm selects a reference frame that has been compensated as mentioned above. For each of the other frames, a displacement field related to the reference frame is generated.[12] The field was calculated using a non-rigid alignment estimator (6-level pyramid image and 100 iterations per pyramid). The displacement field was downgraded to the mean lateral displacement per A-line, and then used to resample all the A-lines of the original sectorized image.

3. RESULTS

3.1 Distortion analysis

Ex-vivo OCT images of swine esophagus were acquired in circumferential imaging mode, at 500 frames/s imaging speed and 15 mm/s pullback speed. The capsule was connected to a 1.5 MHz Fourier Domain Mode Locked OCT system. Right after, sector images were acquired every 30° at 50 frames/s. Fig. 5(a) shows a 2D OCT cross-sectional image, in which the morphological structure of the esophagus is identifiable and no wire shadow was observed. Even though the circumferential image and sectorized image show similar structural features [Fig. 5(b and c)], distortion artifacts during sector scanning can still be seen.

The experimental results of speed measurement [Fig. 5(d)] shows an identifiable and repeatable parabolic speed pattern: static on the limits of the scanning range and reaching maximum speed around the center. This pattern is nonetheless specific for each sector, depending on the range and location of the scanning operation. This speed distortion is considered to be the source of the image distortion. Since the A-scan rate of the OCT system was set to a constant value of 1.5 MHz, a lower motor speed will result in an oversampling of A-lines, more notably close to the edges of the OCT image.

Distortion analysis using speckle decorrelation methods was linked to the motor velocity and the image distortion. Analysis of the results from a single sector [Fig. 5(c)] reveals that the feature of the relative speed profile [Fig. 5(e)] corresponds to that of the measured speed profile [Fig. 5(d)]. They both follow an identifiable pattern related to the actual spatial sampling of the capsule. The results show that the image distortion is due to non-uniform velocity of the micromotor.

3.2 Compensated sector imaging

Using the relative speed profile, a reference frame was created by resampling the A-lines to achieve uniform angular space. The reference frame before and after applying the compensation is presented in Fig. 6. The dotted boxes from Fig. 6(a and b) correspond to the same region of the tissue, while the latter shows lower redundancy of A-lines, after the compensation. Based on the reference frame, image processing distortion compensation was applied to multiple frames. As shown in Fig. 6(d and e), distortion of a further frame was significantly reduced after the image processing compensation. It is also noticeable that the image features after compensation are very close to the original circumferential image as in Fig. 6(c and e). A stable video [Fig. 6(d-e)] was finally achieved, in which lateral distortion is significantly depressed using our image processing method.
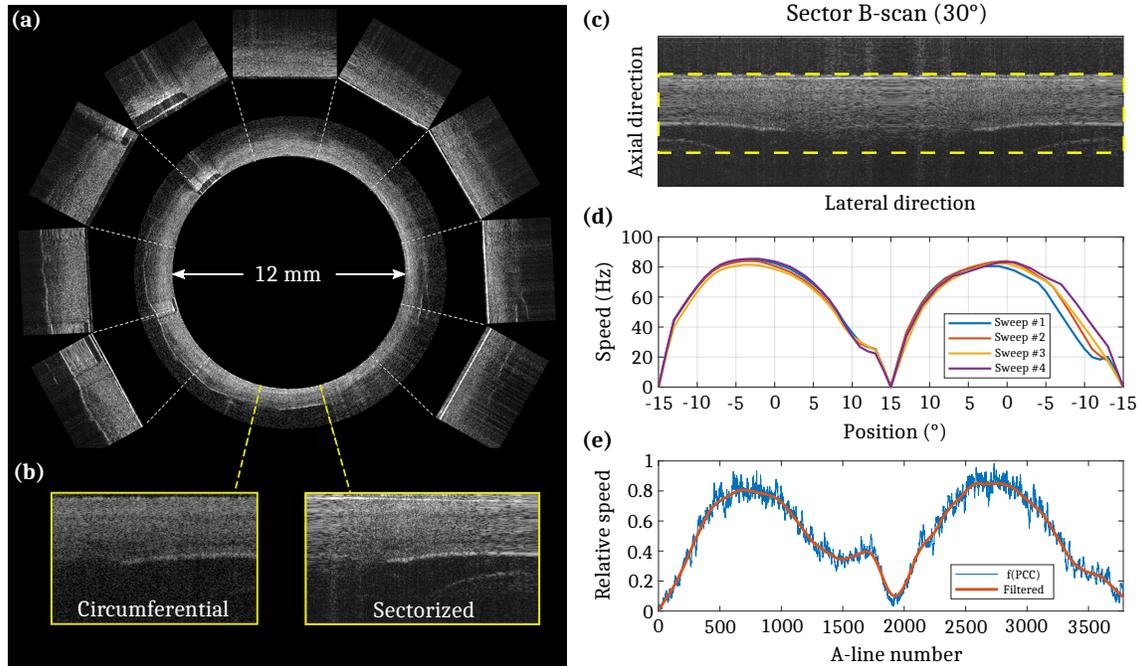
Figure 5. **Capsule imaging results and analysis**. (a) Comparison of an OCT image using circumferential (inner scan) and 30° sector imaging (outer scan) of swine esophagus; (b) Rectangular OCT images of the same sector using circumferential and sectorized imaging; (c) OCT image acquired during a single sweep; (d) Speed profile of the motor at the same location than (c); (e) Speed profile derived from image analysis of the OCT image from (c).
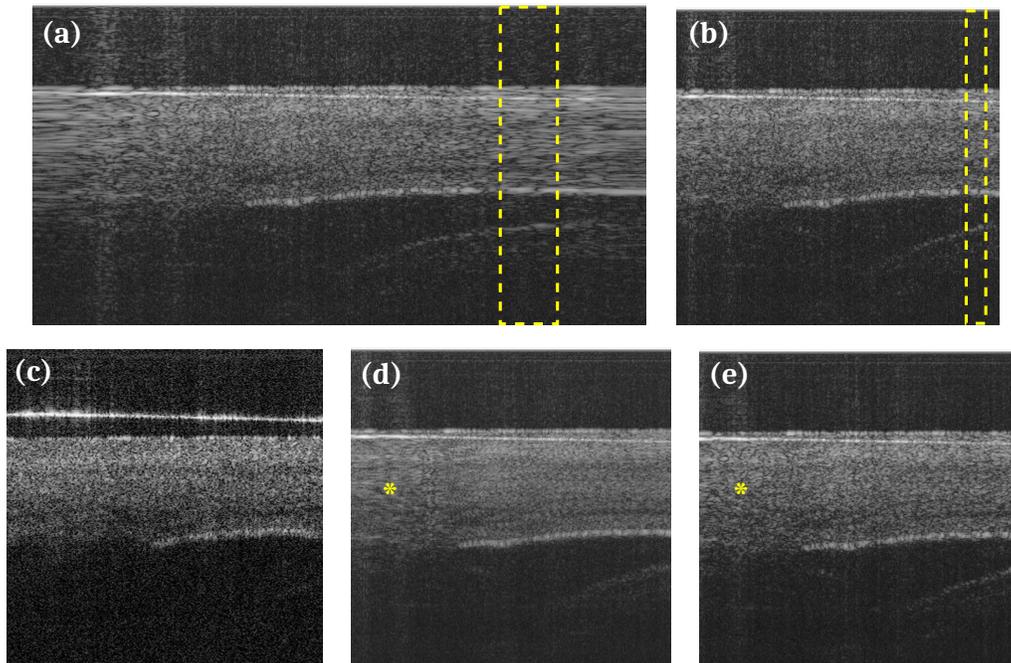
Figure 6. **Distortion compensation results**. (a) Original sector image with non-uniform angular space; (b) Result image after the speed distortion compensation; (c) Analogous circumferential imaging section; (d-e) **Video 1**. Comparison of consecutive blended frames before (d) and after (e) compensating the initial misalignment (see star marks and video) http://dx.doi.org/10.1117/12.2545689.1

4. DISCUSSION

Previously, we presented a shadow-free motorized capsule that offers accurate beam positioning and sector imaging of the esophagus. In this study, we analyzed the image distortion of the sector imaging mode. A repeatable speed pattern of the micromotor is found to be the source of the distortion. We compensated the distortion artifact by resampling the A-lines in a reference frame and aligning all the other frames with the reference frame. A stable sector imaging with much less distortion was finally achieved. As implemented, the compensation method takes approximately 3 seconds for one frame, and therefore cannot be applied in real time. In the next step, we will optimize the algorithm towards real time compensation, i.e: improving the accuracy and reducing the computational cost. We will also further minimize the capsule size and perform pre-clinical and clinical validation of the capsule.

5. CONCLUSION

In this study, we present a shadow-free OCT capsule that performs circumferential imaging, holds the beam steadily and offers sectorized imaging. Distortion introduced during sector imaging was analyzed and compensated. With stable sectorized imaging, we believe that the capsule can potentially be used as a clinical tool in future gastrointestinal endoscopy.

REFERENCES

[1] Huang, D., Swanson, E. A., Lin, C. P., Schuman, J. S., Stinson, W. G., Chang, W., Hee, M. R., Flotte, T., Gregory, K., Puliafito, C. A., and Fujimoto, J. G., "Optical coherence tomography," *Science* **254**(5035), 1178–81 (1991).

[2] Tearney, G. J., Brezinski, M. E., Bouma, B. E., Boppart, S. A., Pitris, C., Southern, J. F., and Fujimoto, J. G., "In vivo endoscopic optical biopsy with optical coherence tomography," *Science* **276**(5321), 2037–9 (1997).

[3] Seibel, E. J., Carroll, R. E., Dominitz, J. A., Johnston, R. S., Melville, C. D., Lee, C. M., Seitz, S. M., and Kimmey, M. B., "Tethered capsule endoscopy, a low-cost and high-performance alternative technology for the screening of esophageal cancer and b.e.," *IEEE Trans Biomed Eng* **55**(3), 1032–42 (2008).

[4] Gora, M. J., Sauk, J. S., Carruth, R. W., Gallagher, K. A., Suter, M. J., Nishioka, N. S., Kava, L. E., Rosenberg, M., Bouma, B. E., and Tearney, G. J., "Tethered capsule endomicroscopy enables less invasive imaging of gastrointestinal tract microstructure," *Nat Med* **19**(2), 238–40 (2013).

[5] Liang, K., Traverso, G., Lee, H. C., Ahsen, O. O., Wang, Z., Potsaid, B., Giacomelli, M., Jayaraman, V., Barman, R., Cable, A., Mashimo, H., Langer, R., and Fujimoto, J. G., "Ultrahigh speed en face oct capsule for endoscopic imaging," *Biomed Opt Express* **6**(4), 1146–63 (2015).

[6] Li, K., Liang, W., Mavadia-Shukla, J., Park, H. C., Li, D., Yuan, W., Wan, S., and Li, X., "Super-achromatic oct capsule for ultrahigh-resolution imaging of esophagus," *J Biophotonics* **12**(3) (2019).

[7] Liang, C. P., Dong, J., Ford, T., Reddy, R., Hosseiny, H., Farrokhi, H., Beatty, M., Singh, K., Osman, H., Vuong, B., Baldwin, G., Grant, C., Giddings, S., Gora, M. J., Rosenberg, M., Nishioka, N., and Tearney, G., "Optical coherence tomography-guided laser marking with tethered capsule endomicroscopy in unsedated patients," *Biomed Opt Express* **10**(3), 1207–1222 (2019).

[8] Lopez-Marin, A., Springeling, G., Beurskens, R., van Beusekom, H., van der Steen, A. F. W., Koch, A. D., Bouma, B. E., Huber, R., van Soest, G., and Wang, T., "Motorized capsule for shadow-free oct imaging and synchronous beam control," *Opt Lett* **44**(15), 3641–3644 (2019).

[9] Liu, X., Huang, Y., and Kang, J. U., "Distortion-free freehand-scanning oct implemented with real-time scanning speed variance correction," *Optics Express* **20**(15), 16567–16583 (2012).

[10] Uribe-Patarroyo, N. and Bouma, B. E., "Rotational distortion correction in endoscopic optical coherence tomography based on speckle decorrelation," *Opt Lett* **40**(23), 5518–21 (2015).

[11] Wang, T., Lancee, C., Beurskens, R., Meijer, J., Knapen, B., van der Steen, A. F. W., and van Soest, G., "Development of a high-speed synchronous micro motor and its application in intravascular imaging," *Sensors and Actuators A - Physical* **218**, 60–68 (2014).

[12] Modersitzki, J., [*Numerical methods for image registration*], Oxford University Press, New York (2004).